

See discussions, stats, and author profiles for this publication at: <https://www.researchgate.net/publication/262015301>

# Antroquinonol D, Isolated from *Antrodia camphorata*, with DNA Demethylation and Anticancer Potential

ARTICLE in JOURNAL OF AGRICULTURAL AND FOOD CHEMISTRY · MAY 2014

Impact Factor: 2.91 · DOI: 10.1021/jf4056924 · Source: PubMed

---

CITATIONS

5

READS

79

---

## 9 AUTHORS, INCLUDING:



[Yu-Jia Chang](#)

Taipei Medical University

81 PUBLICATIONS 1,247 CITATIONS

[SEE PROFILE](#)



[Yi-Ching Wang](#)

National Cheng Kung University

120 PUBLICATIONS 2,524 CITATIONS

[SEE PROFILE](#)



[Yuan-Soo Ho](#)

Taipei Medical University

124 PUBLICATIONS 3,335 CITATIONS

[SEE PROFILE](#)



[Ruo-kai Lin](#)

Taipei Medical University

16 PUBLICATIONS 676 CITATIONS

[SEE PROFILE](#)

## Antroquinonol D, Isolated from *Antrodia camphorata*, with DNA Demethylation and Anticancer Potential

Sheng-Chao Wang,<sup>†</sup> Tzong-Huei Lee,<sup>†,‡</sup> Chun-Hua Hsu,<sup>§</sup> Yu-Jia Chang,<sup>||</sup> Man-Shan Chang,<sup>†</sup> Yi-Ching Wang,<sup>†</sup> Yuan-Soo Ho,<sup>#</sup> Wu-Che Wen,<sup>▽</sup> and Ruo-Kai Lin<sup>\*,†,‡,||</sup>

<sup>†</sup>Graduate Institute of Pharmacognosy, Taipei Medical University, 250 Wu-Hsing Street Taipei, TW 110, Taiwan, R. O. C.

<sup>‡</sup>Ph.D. Program for the Clinical Drug Discovery from Botanical Herbs, Taipei Medical University, 250 Wu-Hsing Street Taipei, TW 110, Taiwan, R. O. C.

<sup>§</sup>Department of Agricultural Chemistry, National Taiwan University, No. 1, Sec. 4, Roosevelt Road Taipei, TW 10617, Taiwan, R. O. C.

<sup>||</sup>Graduate Institute of Clinical Medicine, College of Medicine, Taipei Medical University, 250 Wu-Hsing Street Taipei, TW 110, Taiwan, R. O. C.

<sup>#</sup>Department of Pharmacology and Institute of Basic Medical Sciences, National Cheng Kung University, No.1, University Road, Tainan, TW 701, Taiwan, R.O.C.

<sup>\*</sup>Graduate Institute of Biomedical Technology, Taipei Medical University, Taipei, TW 110, Taiwan, R. O. C.

<sup>▽</sup>Golden Biotechnology Corporation, 15F., No.27-6, Sec. 2, Zhongzheng E. Rd, Taipei, TW 110, Taiwan, R.O.C.

<sup>†</sup>Master Program for Clinical Pharmacogenomics and Pharmacoproteomics, Taipei Medical University, 250 Wu-Hsing Street Taipei, TW 110, Taiwan, R. O. C.

### S Supporting Information

**ABSTRACT:** DNA methyltransferase 1 (DNMT1) catalyzes DNA methylation and is overexpressed in various human diseases, including cancer. A rational approach to preventing tumorigenesis involves the use of pharmacologic inhibitors of DNA methylation; these inhibitors should reactivate tumor suppressor genes (TSGs) in tumor cells and restore tumor suppressor pathways. Antroquinonol D (3-demethoxyl antroquinonol), a new DNMT1 inhibitor, was isolated from *Antrodia camphorata* and identified using nuclear magnetic resonance. Antroquinonol D inhibited the growth of MCF7, T47D, and MDA-MB-231 breast cancer cells without harming normal MCF10A and IMR-90 cells. The SRB assay showed that the 50% growth inhibition (GI<sub>50</sub>) in MCF7, T47D, and MDA-MB-231 breast cancer cells following treatment with antroquinonol D was 8.01, 3.57, and 25.08  $\mu$ M, respectively. D-Antroquinonol also inhibited the migratory ability of MDA-MB-231 breast cancer cells in wound healing and Transwell assays. In addition, antroquinonol D inhibited DNMT1 activity, as assessed by the DNMT1 methyltransferase activity assay. As the cofactor SAM level increased, the inhibitory effects of D-antroquinonol on DNMT1 gradually decreased. An enzyme activity assay and molecular modeling revealed that antroquinonol D is bound to the catalytic domain of DNMT1 and competes for the same binding pocket in the DNMT1 enzyme as the cofactor SAM, but does not compete for the binding pocket in the DNMT3B enzyme. An Illumina Methylation 450 K array-based assay and real-time PCR assay revealed that antroquinonol D decreased the methylation status and reactivated the expression of multiple TSGs in MDA-MB-231 breast cancer cells. In conclusion, we showed that antroquinonol D induces DNA demethylation and the recovery of multiple tumor suppressor genes, while inhibiting breast cancer growth and migration potential.

**KEYWORDS:** breast cancer, DNA methyltransferase, DNA methylation, *Antrodia camphorata*, tumor suppressor genes, cell migration

### INTRODUCTION

The wild natural fruiting body of *Antrodia camphorata* has long been used by aboriginal peoples to treat hepatitis, cirrhosis and liver cancer and has been used in Taiwan to cure diarrhea, abdominal pain, hypertension, itching of the skin and liver cancer.<sup>1</sup> Due to its extremely slow growth rate and high host specificity for the endangered tree *Cinnamomum kanehira* Hay (Lauraceae), the fruiting body cannot be mass-produced for commercialization. Therefore, the mycelium of *A. camphorata* has recently been developed by industrial companies as a health food and has been reported to have antitumor effects.<sup>2,3</sup> The process of tumorigenesis is initiated and promoted by molecular abnormalities, including oncogene activation and

tumor suppressor gene (TSG) inactivation.<sup>4</sup> Down-regulation of tumor suppressor genes (TSGs) by 5' CpG island hypermethylation is an important event in tumor development.<sup>5</sup> CpG island hypermethylation inactivates TSGs and is a major epigenetic modification of the mammalian genome that is not accompanied by changes in the DNA sequence.<sup>6</sup> Aberrant promoter hypermethylation of TSG-associated CpG islands can lead to transcriptional silencing and result in tumorigenesis.<sup>7</sup>

Received: December 23, 2013

Revised: March 18, 2014

Accepted: April 28, 2014

Published: May 1, 2014



DNA methylation disorders give rise to several significant human diseases, including various cancers, neurological disorders, psychosis and cardiovascular diseases, many of which are mediated by altered DNA methyltransferase 1 (DNMT1) expression and activity.<sup>8–12</sup> Previous reports have indicated that DNMT1 is overexpressed in lung, hepatocellular, colorectal, gastric and breast tumors, as well as acute and chronic myelogenous leukemias.<sup>13–18</sup> Abnormal expression of DNMT1 in vivo induces cellular alterations such as transformation, whereas inhibition of DNMT1 expression or activity results in the reversal of fos transformation.<sup>19</sup> The inhibition of DNA methyltransferase (DNMT), the enzyme that methylates the cytosine residues of CpG islands, may inhibit or reverse the process of epigenetic silencing.<sup>10</sup> Therefore, the use of pharmacologic inhibitors of DNA methylation represents an attractive, rational approach to the reversal of epigenetic TSG silencing. These inhibitors will hopefully reactivate TSGs in tumors and restore activity in critical cellular pathways.

Several DNMT inhibitors have exhibited potent antitumor activities in human xenograft models, indicating their potential usefulness as new cancer therapeutic agents. The first extensively studied DNMT inhibitors were 5-azacytidine (Vidaza) and 5-aza-2'-deoxycytidine (decitabine), which have been approved by the US Food and Drug Administration (FDA) for the treatment of myelodysplastic syndrome. However, these inhibitors induced hematopoietic toxicity and neutropenia in clinical trials.<sup>20–22</sup> Some non-nucleoside drugs and natural compounds, such as epigallocatechin-3-gallate (EGCG), RG108, mithramycin A and procaine, have also been reported to inhibit DNMT activity.<sup>23,24</sup> However, 5-aza-2'-deoxycytidine and EGCG were found to be genotoxic,<sup>25</sup> and mithramycin A has been observed to cause marked hemorrhagic toxicity in patients.<sup>26</sup> Procaine and EGCG failed to induce significant genomic DNA demethylation in some of the tested cell lines.<sup>25</sup> Therefore, other effective, minimally toxic DNMT inhibitors could potentially be developed to provide additional DNMT inhibitors for clinical use.

In the present study, we discovered that a ubiquinone derivative, antroquinonol D, may act as a DNMT1 inhibitor. Antroquinonol D, isolated from the mycelium of *Antrodia camphorata* (*A. camphorata*), can inhibit DNMT1 enzyme activity, induce the re-expression of multiple tumor suppressor genes, increase cancer cell death without harming normal cells, and inhibit the migratory ability of MDA-MB-231 breast cancer cells.

## MATERIALS AND METHODS

**Isolation of Antroquinonol D.** The culture conditions of *A. camphorata* and the extraction method of antroquinonol D were performed as previously reported.<sup>2</sup> From 500 g dried powder of cultured *A. camphorata* mycelium, 9.6 mg of antroquinonol D was obtained. <sup>1</sup>H- and <sup>13</sup>C NMR of antroquinonol D were acquired using a Bruker DMX-500 SB spectrometer (Ettlingen, Germany). Mass spectra were obtained using a Thermo Finnigan LCQ-Duo spectrometer (Waltham, MA). The following data were recorded for 3-demethoxy antroquinonol (Figure 1): slight yellowish oil;  $[\alpha]^{23}_D: +52.2$  (*c* 0.5, MeOH); <sup>1</sup>H NMR data (CD<sub>3</sub>OD, 500 MHz):  $\delta_H$  5.91 (1H, d, *J* = 5.6 Hz, H-3), 5.21 (1H, t, *J* = 7.3 Hz, H-8), 5.10 (1H, t, *J* = 6.9 Hz, H-12), 5.09 (1H, t, *J* = 7.2 Hz, H-16), 4.48 (1H, dd, *J* = 5.6, 3.7 Hz, H-4), 3.59 (3H, s, H<sub>3</sub>-23), 2.67 (1H, m, H-6), 2.26–1.95 (10H, H<sub>2</sub>-7, -10, -11, -14 and -15), 1.78 (1H, m, H-5), 1.65 (3H, s, H<sub>3</sub>-18), 1.62 (3H, s, H<sub>3</sub>-

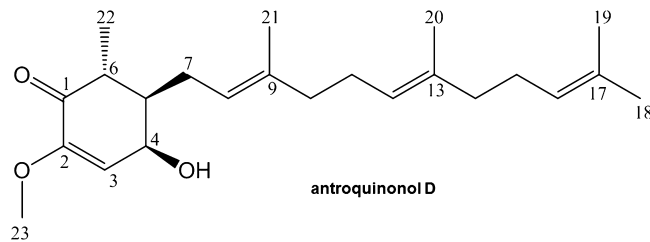


**Figure 1.** Structure of antroquinonol D. Antroquinonol D, a ubiquinone derivative, was isolated from the solid-state fermented mycelium of *Antrodia camphorata* (Polyporaceae, Aphylophorales), a parasitic fungus that is indigenous to Taiwan. The structure of antroquinonol D is completely different from that of other non-nucleoside DNMT inhibitors, such as epigallocatechin-3-gallate (EGCG), RG108, mithramycin A and procaine.

21), 1.60 (3H, s, H<sub>3</sub>-20), 1.57 (3H, s, H<sub>3</sub>-19), 1.16 (3H, d, *J* = 6.9 Hz, H<sub>3</sub>-22); <sup>13</sup>C NMR data (CD<sub>3</sub>OD, 125 MHz):  $\delta_C$  198.7 (C-1), 152.0 (C-2), 138.1 (C-9), 136.0 (C-13), 132.1 (C-17), 125.5 (C-16), 125.3 (C-12), 123.3 (C-8), 116.6 (C-3), 65.0 (C-2), 55.3 (C-23), 47.5 (C-5), 43.4 (C-6), 41.0 (C-10), 40.9 (C-14), 28.2 (C-7), 27.8 (C-15), 27.4 (C-11), 25.9 (C-18), 17.8 (C-19), 16.3 (C-21), 16.2 (C-20), 13.1 (C-22); ESI-MS: *m/z* = 383 [M + Na]<sup>+</sup>; HR-ESI-MS: *m/z* = 383.2560 [M + Na]<sup>+</sup>; calculated for C<sub>23</sub>H<sub>36</sub>O<sub>3</sub> + Na<sup>+</sup>: 383.2562.

**Molecular Modeling and Docking.** For the molecular docking experiments, the amino acid sequence of the DNMT1 catalytic domain was used as the query to perform a BLAST search against the RCSB Protein Data Bank. The crystal structure of DNMT1 in complex with sinefungin (PDB code 3SWR) was used to rebuild the model of the human DNMT1 catalytic domain. The DNMT3B catalytic domain was modeled using the crystal structure of DNMT3A (PDB code 2QRV) as a template. The structure was validated using Profile3D and PROCHECK. AutoDockTools 1.5.4 was used to prepare the pdbqt files for the ligands/protein and the control-parameter file for gridding and docking.<sup>27</sup> Autodock 4.2 was used to implement the docking process and calculate the binding energies.<sup>28</sup> The Autodock program software uses Monte Carlo-simulated annealing and a Lamarckian genetic algorithm to create a set of possible conformations. All of the ligand bonds were set to be rotatable. A grid box with a dimension of 50 × 80 × 50 points and default grid spacing of 0.375 Å was set around the active sites, covering the DNA-binding region and allowing ligands to move freely. Grid maps were generated using the Autogrid program. The best conformation was defined as the one with the lowest docked energy after the docking search had been completed. The interactions of the protein/ligand complex, including hydrogen bonds and bond lengths, were analyzed using Pymol.

**DNMT1 and DNMT3B Methyltransferase Activity Assays.** The drug screening was performed using a DNA Methyltransferase 1 Activity/Inhibitor Screening Assay Kit (Abnova). One hundred nanograms of the DNMT1 enzyme and the indicated concentrations of the potential DNMT inhibitors were added into a CpG-enriched DNA-coated 96-well plate and incubated for 2 h. The DNMT1 enzyme transfers a methyl group to cytosine from S-adenosyl methionine (SAM), thereby methylating the DNA substrate. The methylated DNA can be recognized using an anti-5-methylcytosine antibody. The ratio or amount of methylated DNA, which is proportional to the enzyme activity, can then be colorimetrically quantified using an ELISA-like reaction. Finally,

we detected the colorimetric reaction (OD450 nm) using an ELISA reader. The inhibitory effects of all of the drugs were calculated as follows: The relative DNMT1 activity (%) = (the OD450 of the sample-the OD450 of the blank)/(the OD450 of the DMSO control-the OD450 of the blank) × 100. To further confirm the specificity and underlying mechanism of the antroquinonol D-mediated DNMT inhibition, we measured the DNMT1 (Active Motif) and DNMT3B (BPS Bioscience, San Diego, CA) enzyme activity in the presence of 40, 80, or 160 μM of SAM following antroquinonol D, antroquinonol or EGCG (Sigma-Aldrich) treatment using an EpiQuik DNA Methyltransferase (DNMT) Activity/Inhibition Assay Kit (Epigentek, Farmingdale, NY). The key principles, methodology and protocols are similar to the DNA Methyltransferase 1 Activity/Inhibitor Screening Assay Kit. Antroquinonol D and antroquinonol were provided by Golden Biotechnology Corporation.

**Cell Lines and Drug Treatments.** The MCF7, T47D and MDA-MB-231 breast cancer cell lines were obtained from the Bioresource Collection and Research Center (BCRC, Hsinchu, Taiwan). MCF10A, a normal mammary gland cell line, was obtained from the American Tissue Cell Culture collection. IMR-90, a normal fibroblast-like cell line that was established from the lung tissue of a female fetus, was obtained from the BCRC. The MCF7, MDA-MB-231 and IMR-90 cell lines were cultured in DMEM (Invitrogen) supplemented with 10% fetal bovine serum and 1% penicillin/streptomycin. The T47D cell line was cultured in RPMI 1640 (Invitrogen) that had been supplemented with 10% fetal bovine serum and 1% penicillin/streptomycin. The cells were treated with DMSO, antroquinonol D, or the DNMT inhibitors 5-azacytidine (AZA) and decitabine (DAC) for the indicated durations. Antroquinonol D was dissolved in DMSO. AZA (Sigma-Aldrich) and DAC (Sigma-Aldrich) were dissolved in acetic acid/water (1:1).

**Sulphorhodamine B (SRB) Assays.** A sulphorhodamine B (SRB) assay was used to determine the cell growth rate. Based on the growth curves of the MCF7, T47D, MDA-MB-231, MCF10A and IMR-90 cell lines, the cells were seeded in 96-well plates at densities of 5000, 8000, 3000, 2000, and 6000 cells/well, respectively, and incubated with the indicated drugs for 3 days. Additionally, MCF7, T47D, MDA-MB-231, MCF10A and IMR-90 cells were seeded in 96-well plates at densities of 3000, 5000, 750, 500, and 4000 cells/well, respectively, and incubated with the indicated drugs for 6 days. The growth curves of the MCF7, T47D, MDA-MB-231, MCF10A and IMR-90 cell lines over 6 days are shown in Figure S1, Supporting Information. The cells were fixed with 10% trichloroacetic acid at the indicated times. Cell growth was assessed via OD determination at 515 nm using a microplate reader. The data for antroquinonol D were normalized to its solvent control (DMSO). The 5-azacytidine (AZA) and decitabine (DAC) data were also normalized to their solvent controls (50% acetic acid). The solvent controls were added in the same amounts as those used for the treatment drugs at the indicated concentrations. The growth inhibition rates were calculated using the following equation: Cell growth inhibition rate (%) = 100 - [(Ti - Tz)/(C - Tz)] × 100 (Ti ≥ Tz). Cytotoxicity rate (%) = [(Tz - Ti)/Tz] × 100 (Tz ≥ Ti). Ti = the OD of the inhibitor sample. Tz = the OD of the basal cells. C = the OD of the control.

**MTT Assays.** The cells were seeded in 96-well microtiter plates (100 μL/well) at densities of 5000 cells/well and grown in culture medium. The next day, the culture medium was

replaced with 100 μL of culture medium containing different concentrations of DMSO or a DNMT1 inhibitor, and cell viability was assayed using an MTT assay (3-(4,5-dimethylthiazol-2yl)-2,5-diphenyltetrazolium bromide) after 72 h of incubation. Cell viability was assessed using OD determinations at 570 nm using a microplate reader. MTT powder (Sigma-Aldrich) was dissolved in phosphate-buffered saline at 3.3 mg/mL and filtered.<sup>29</sup>

#### Wound Healing Assays for Migration Analyses.

Treated and untreated cells were plated at densities of  $2 \times 10^5$  cells in 10 cm culture dishes in quadruplicate and incubated at 37 °C. After the cells had been treated with 15 μM antroquinonol D for 6 days, wound healing assays were performed using Culture-Inserts (Ibidi). Cell-free gaps of 500 μm were created after removing the Culture-Inserts. After seeding the cells overnight, the Culture-Inserts were removed, and images of the wounded areas were acquired using an inverted microscope (Nikon) at the indicated time points. The percentage of closure of the wounded area was measured and analyzed using ImageJ software, and the migratory ability was calculated.

#### Transwell Assays for Migration Analyses.

The Transwell consists of upper and lower chambers that are separated by a layer of membrane that has a pore size of 8 μm (Falcon). Approximately  $2 \times 10^4$  treated and untreated MDA-MB-231 cells were seeded onto the upper chambers with 300 μL of serum-free medium containing drugs, and 800 μL of DMEM containing 10% FBS was added to the lower chambers as a chemoattractant. The seeded cells were incubated for 16 h. The cells that did not invade were removed using a scraper and washed twice with PBS, then fixed and stained using 1% crystal violet/ddH<sub>2</sub>O for 60 min at room temperature. Five random views were photographed under a microscope (Nikon) and then counted and quantified using ImageJ.

#### Cell Migration Assays Using the xCELLigence Bio-sensor System.

Migration assays were performed using the RTCA DP instrument (Roche Diagnostics GmbH, Germany), which was placed in a humidified incubator and maintained at 5% CO<sub>2</sub> and 37 °C, as previously described.<sup>30</sup> The cells were seeded into specifically designed 16-well plates (CIM-plate 16, Roche Diagnostics GmbH) that had 8 μm pores that were similar to conventional Transwells and contained micro-electrodes on the undersides of the upper chamber's membranes. The cells (20 000 cells/well) were seeded into the upper chambers in serum-free medium, and media containing 10% FBS was added to the lower chambers. Each sample was treated under the same conditions in four independent wells. The CIM-plate 16 was monitored every 10 s for 40 min and once every hour thereafter. The greater the number of cells attached to the electrodes, the larger the increases in electrode impedance. The electrode impedance, which was displayed and recorded as the Cell Index (CI) value, reflected the biological statuses of the monitored cells, including the cell numbers, viabilities, morphologies and degrees of adhesion. The data analyses were performed using the RTCA software program v1.2, which was supplied with the instrument. The *t* test was to analyze the data differences.

#### DNA and RNA Extractions.

Genomic DNA from the cell lines was prepared using the Blood and Tissue Genomic DNA Extraction Miniprep System (Viogene, Sunnyvale, CA). Total mRNA was extracted from the cells using the TRIzol reagent (Invitrogen). The DNA and RNA were quantified, and the

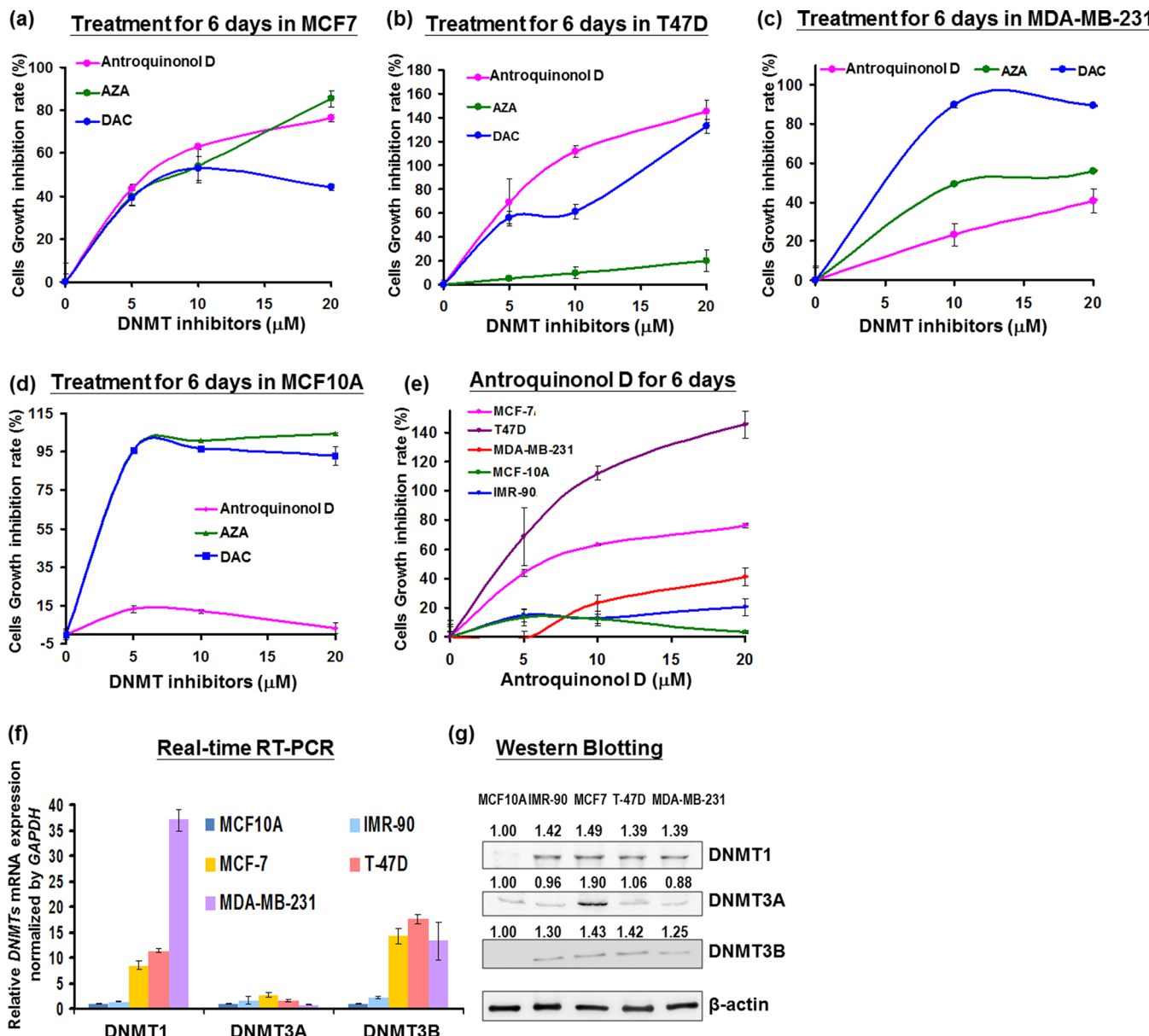


**Figure 2.** Growth of the breast cancer cell lines MCF7, T47D, MDA-MB-231 and the normal cell line MCF10A and IMR-90 following treatment with DNMT1 inhibitors. The growth of the MCF7 (a), T47D (b) and MDA-MB-231 (c) cancer cell lines, the MCF10A normal mammary gland cells, and the IMR-90 normal lung cell line (d and e), was determined using the SRB assay after the cells had been treated with antroquinonol D or the DNMT inhibitor azacitidine (AZA) and decitabine (DAC) at the indicated concentrations for 6 days. Cell growth inhibition rate (%) =  $100 - [(Ti - Tz)/(C - Tz)] \times 100$  ( $Ti \geq Tz$ ).  $Ti$  = the OD of the inhibitor sample;  $Tz$  = the OD of the basal cells;  $C$  = the OD of the control. The cytotoxic effects of antroquinonol D in normal MCF10A and IMR-90 cells were lower than those of AZA and DAC after 6 days of treatment. (f) DNMT1, DNMT3A and DNMT3B mRNA expression levels were analyzed using real-time RT-PCR and were normalized to GAPDH. (g) DNMT1, DNMT3A and DNMT3B protein expression levels were analyzed using Western blotting. The data are presented as the means  $\pm$  s.d. All experiments were performed with at least two biological duplicates and three technical replicates.

purities were verified by measuring the  $A_{260}$  and  $A_{260}/A_{280}$  ratios (which ranged from 1.8 to 2.0).

**DNA Methylation Assays.** The DNA methylation statuses of the MDA-MB-231 cells were determined following treatment with 15  $\mu$ M antroquinonol D for 6 days. Five hundred nanograms of genomic DNA were bisulfite-converted using an EZ Methylation Gold kit (Zymo Research, Irvine, CA) according to the manufacturer's recommended protocol. The DNA methylation analyses were performed using Illumina Methylation 450 K array-based assays (Illumina, San Diego, CA). The array analyses were performed by Health GeneTech Corporation, Taiwan. Methylation scores for each CpG site

were classified as "Beta" values that ranged from 0 (unmethylated) to 1 (fully methylated) by determining the ratios of the methylated signal intensities to the sums of the methylated and unmethylated signal outputs. Functional annotation clustering of differentially demethylated genes was performed using Functional DAVID Bioinformatics Resources 6.7.<sup>31</sup> Supporting Information Figure S9 was generated using XMind 3.2.1. The methylation patterns of the *FANCC* and *CACNA1A* genes were further confirmed and quantified using pyrosequencing. Because no primers were found that could be used for pyrosequencing that targeted the DNA regions of the *FANCC* and *CACNA1A* genes (which were detected using the

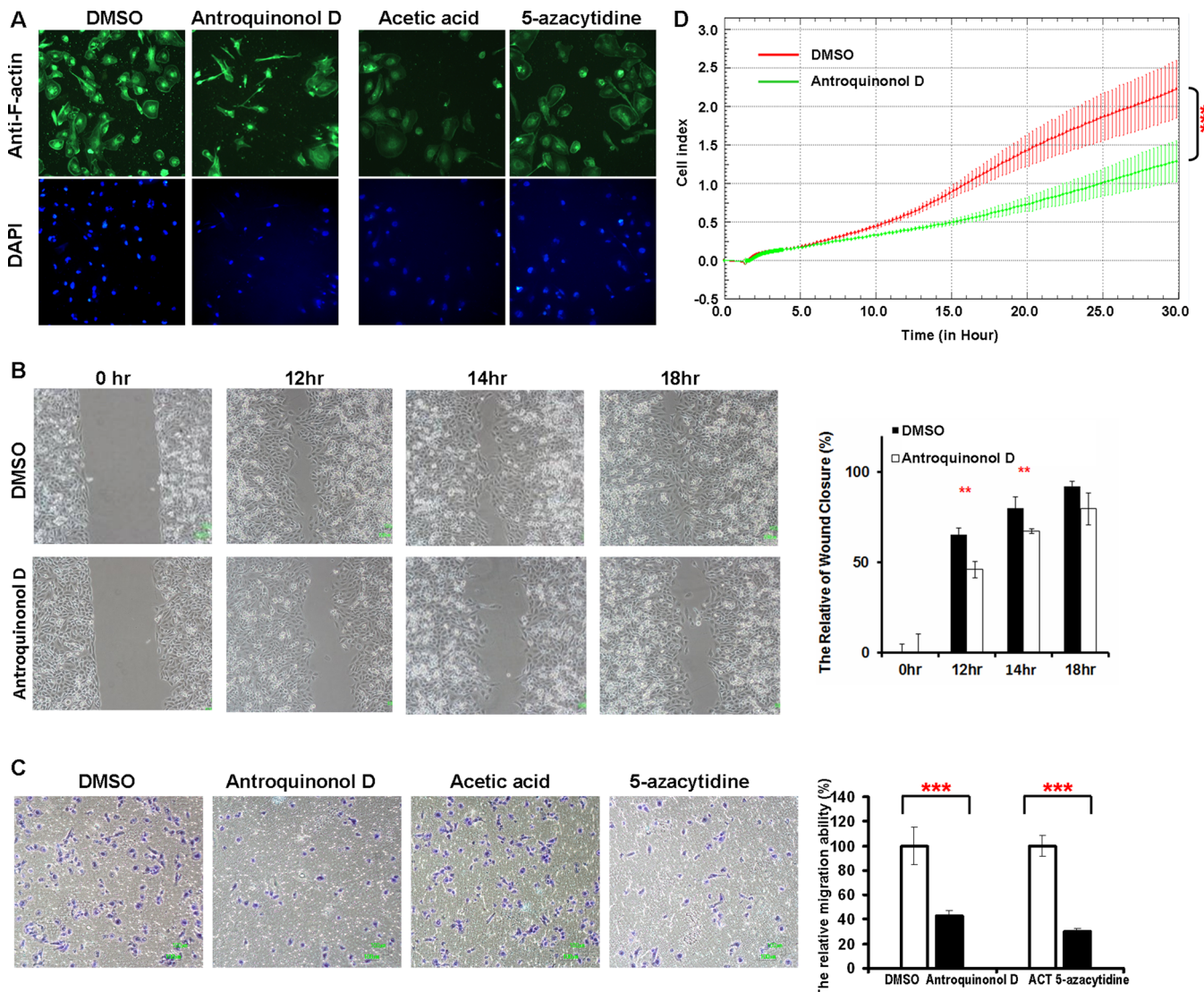


**Figure 3.** Antroquinonol D inhibits the migration of MDA-MB-231 breast cancer cells. (a) The distribution of F-actin (green) was detected by immunofluorescence staining and fluorescence microscopy using anti-F-actin antibody (original magnification 200X). DAPI was used to label cell nuclei (blue). (b) Wound healing was determined using a Culture-Insert assay to analyze the migratory abilities of the cells. The cells were photographed at 0, 12, 14, and 18 h. The images represent the untreated (upper panel) and treated (lower panel) cells (original magnification  $\times 100$ ). The data indicate that antroquinonol D decreased the migration of MDA-MB-231 cells compared to the DMSO control. The experiment was performed with at least two biological duplicates and three technical replicates. (c) A Transwell assay was used to further investigate the migratory abilities of the cells. The images represent treatment with DMSO, antroquinonol D, acetic acid (the solvent control for 5-azacytidine) or 5-azacytidine (original magnification  $\times 100$ ). The average number of migratory cells (those that passed through the membrane) was counted in five different fields. Antroquinonol D significantly decreased the migration of MDA-MB-231 cells. \*\*\*  $p \leq 0.001$ . The experiment was performed with three technical replicates. (d) Cell migration was also assessed using specifically designed 16-well plates (CIM-plate 16) that had 8  $\mu\text{m}$  pores. The CIM-plate 16 was monitored every 10 s for 40 min and then once every hour. Data analyses were performed using the RTCA software v1.2 program that was supplied with the instrument. The Cell Index (CI) value reflects the biological status of the monitored cells, including the cell number, cell viability, morphology and degree of adhesion. The experiments were performed in technical quadruplicate. The data are presented as the means  $\pm$  s.d. \*\*  $p \leq 0.005$ , \*\*\*  $p \leq 0.001$ . The *t* test was used to calculate group differences in all experiments.

Methylation 450 K array-based assay), we designed primers that were targeted to the promoter regions of the *FANCC* and *CACNA1A* genes for use in the pyrosequencing assay. The primers were designed using the MethPrimer<sup>32</sup> and Methyl Primer Express v1.0 (ABI) software programs. The PCR reactions were performed using biotinylated primers to convert the PCR products to single-stranded DNA templates. The pyrosequencing reactions and methylation quantification were performed using PyroMark Q24, which was provided by the Mission Biotech Corporation, Taiwan. The primers are described in Table S1, Supporting Information.

**Real-time RT-PCR.** The mRNA expression levels were measured by performing real-time RT-PCR using a LightCycler 480 (Roche Applied Science, Mannheim, Germany). Real-time PCR was performed using the LightCycler 480 Probe Master kit (Roche Applied Science) with the specific primers and the corresponding Universal Probe Library probe (Roche Applied Science) according to the manufacturer's instructions. Normalized gene expression values, which were calibrated to the control group, were obtained using the LightCycler Relative Quantification software program (ver. 2.0, Roche Applied

Science). GAPDH was used as a reference gene. The primers are described in Table S1, Supporting Information.

**Cell Lyses and Immunoblotting Analyses.** For Western blotting assays, the cells were lysed on ice in radioimmunoprecipitation buffer (0.05 M Tris-HCl [pH 7.4], 0.15 M NaCl, 0.25% deoxycholic acid, 1% Igepal CA-630, and 1 mM ethylenediaminetetraacetic acid). The lysates were then centrifuged at 13 000 r.p.m. at 4 °C for 10 min. The protein extracts were solubilized in sodium dodecyl sulfate (SDS) gel loading buffer (60 mmol/L Tris base, 2% SDS, 10% glycerol and 5%  $\beta$ -mercaptoethanol). Samples containing equal amounts of protein (40  $\mu$ g) were separated on an 8% SDS-polyacrylamide gel using electrophoresis and electroblotted onto Immobilon-P membranes (Millipore, Bedford, MA) in transfer buffer. Immunoblotting was performed using antibodies that had been raised against DNMT1 (1:1000, GeneTex, TX), DNMT3A (1:1000, Cell Signaling, Danvers, MA), DNMT3B (1:250, Abcam, Cambridge, U.K.), FANCC (1:500, GeneTex, Hsin-Chu, Taiwan), and CACNA1A (1:250, Abcam, Cambridge, U.K.), total AKT (1:1000, Cell Signaling, Danvers, MA), phosphor-AKT Ser473 (1:500, Cell Signaling, Danvers, MA).  $\beta$ -Actin (1:5000, GeneTex, TX) was used as an internal control. For Immunofluorescence staining assays, cells were seeded in 4-well glass chamber slides (Nunc). After DNMT inhibitor treatment, cells were fixed in 4% formaldehyde and stained with anti-F-actin (1:200, Abcam, Cambridge, U.K.) cells. The image was detected by using the Olympus IX71 Inverted Microscope System.

## RESULTS AND DISCUSSION

**Identification of Antroquinonol D.** Antroquinonol D was obtained as a slight yellowish oil. Its molecular formula,  $C_{23}H_{36}O_3$ , was deduced through analysis of the  $^{13}C$  NMR and HRESIMS data. The  $^1H$  NMR spectrum of antroquinonol D exhibited resonances compatible with those of antroquinonol except that a 3-methoxyl group at C-3 was substituted by an olefinic methine signal at  $\delta_H$  5.91 (d,  $J$  = 5.6 Hz, H-3) in antroquinonol D.<sup>2</sup> The difference was also reflected in the  $^{13}C$  NMR of antroquinonol D, in which C-24 disappeared and a quaternary C-3 was replaced by a tertiary C-3 at  $\delta_C$  116.6. Thus, the gross structure of antroquinonol D was determined to be 3-demethoxyl antroquinonol. The relative configuration of cyclohexenone was consistent with that of antroquinonol. The configurations of  $\Delta^8$ ,  $\Delta^{12}$  and  $\Delta^{16}$  were *E* as corroborated by the chemical shifts of C-21, C-20 and C-19 at respective  $\delta_C$  16.3, 16.2, and 17.8. Accordingly, the structure of antroquinonol D is shown in Figure 1. We examined signals and noise in the  $^1H$  NMR spectrum of antroquinonol D, and the purity of antroquinonol D (LTH-0909-1) was determined to be greater than 95% (Supporting Information Figure S2).

**Antroquinonol D Inhibits the Growth of Breast Cancer Cells, but not normal cells.** Clinical toxicity is a major concern for the clinical application of anticancer agents. Therefore, we treated normal cell lines, MCF10A and IMR-90, and three breast cancer cell lines, MCF7, T47D and MDA-MB-231, with the DNMT inhibitor for 3 or 6 days. The drug treatment protocols are described in Supporting Information Figure S3. Antroquinonol D suppressed the growth of MCF7 and T47D cells as effectively as AZA and DAC treatment at 6 days (Figure 2a and Figure 2b). The SRB assay showed that the GI<sub>50</sub> in MCF7, T47D and MDA-MB-231 breast cancer cells following antroquinonol D treatment is 8.01, 3.57, and 25.08  $\mu$ M, respectively. Antroquinonol D could lead to cytotoxic

effects in T47D and MCF7 cells (Figure S4a, Supporting Information). In addition, antroquinonol D treatment displayed lower cytotoxicity to normal mammary gland cells (MCF10A) and human fibroblast cells (IMR-90) than AZA and DAC treatment for 3 days (Figure S4b, Supporting Information) and 6 days (Figure 2d and Figure 2e), respectively. The antroquinonol D-mediated cell growth inhibition and cell death at 72 h, assessed by the MTT assay, was also stronger than that demonstrated by another DNMT inhibitor, EGCG, in MCF7 and NDA-MB-231 cells (Figure S4c, Supporting Information).

**Antroquinonol D Inhibits the Migration of MDA-MB-231 Breast Cancer Cells.** Metastasis is the primary cause of mortality for most cancer patients. The mobility of tumor cells is a key step in the metastatic process. The MDA-MB-231 cells exhibit invasive tumor features with rapid migration ability. The MDA-MB-231 cells are good cell models for analyzing whether antroquinonol D could also inhibit cell migration ability. We observed morphological changes in MDA-MB-231 cells, including cell shrinkage and fragmentation, after antroquinonol D treatment for 6 days (Supporting Information Figure S5 right panel) that were greater than those observed following DMSO treatment (Supporting Information Figure S5 left panel). Dynamic regulation of the filamentous actin (F-actin) cytoskeleton is critical to cell adhesion and migration.<sup>33</sup> Immunofluorescence imaging revealed that the network expansion of F-actin was not as extensive after antroquinonol D treatment as after DMSO control treatment (Figure 3a). Cell motility was further analyzed using wound healing and Transwell assays. The results of the wound healing assays indicated that the MDA-MB-231 cells migrated more slowly when treated with 15  $\mu$ M antroquinonol D for 6 days compared to the DMSO control-treated cells (Figure 3b). The Transwell migration assays also revealed that antroquinonol D decreased the migration ability of MDA-MB-231 cells by 56.9% (Figure 3c). Antroquinonol D and a positive control DNMT inhibitor, AZA, displayed similar suppression effects on the migratory ability of MDA-MB-231 breast cancer cells. To further confirm that the DNMT inhibitor antroquinonol D influenced the migratory ability of breast cancer cells, a migration assay was performed using the xCELLigence biosensor system, and the numbers of cells that migrated were reflected by the cell index. As shown in Figure 3c, the cell indices in the DMSO-treated control cells and antroquinonol D-treated cells were 2.2 and 1.3, respectively, after 30 h. The migratory ability was reduced to approximately 41% in the antroquinonol D-treated cells compared to the DMSO-treated control cells (Figure 3d). These results indicate that this DNMT inhibitor can suppress the migratory ability of MDA-MB-231 breast cancer cells.

**Antroquinonol D Can Inhibit DNMT1 Enzyme Activity.** A previous study reported that antroquinonol induces anticancer activity in human pancreatic cancers through an inhibitory effect on PI3-kinase/Akt/mTOR pathways.<sup>34</sup> In our study, neither antroquinonol nor antroquinonol D can inhibit Akt phosphorylation in MDA-MB-231 cells (Supporting Information Figure S6), suggesting that the anticancer effect mediated by antroquinonol D is mediated through another pathway. Down-regulation of tumor suppressor genes (TSGs) by 5' CpG island hypermethylation is an important event in tumor growth and progression.<sup>5</sup> Blocking DNA methyltransferase (DNMT) could potentially inhibit or reverse the process of epigenetic silencing. To develop a new DNMT inhibitor and

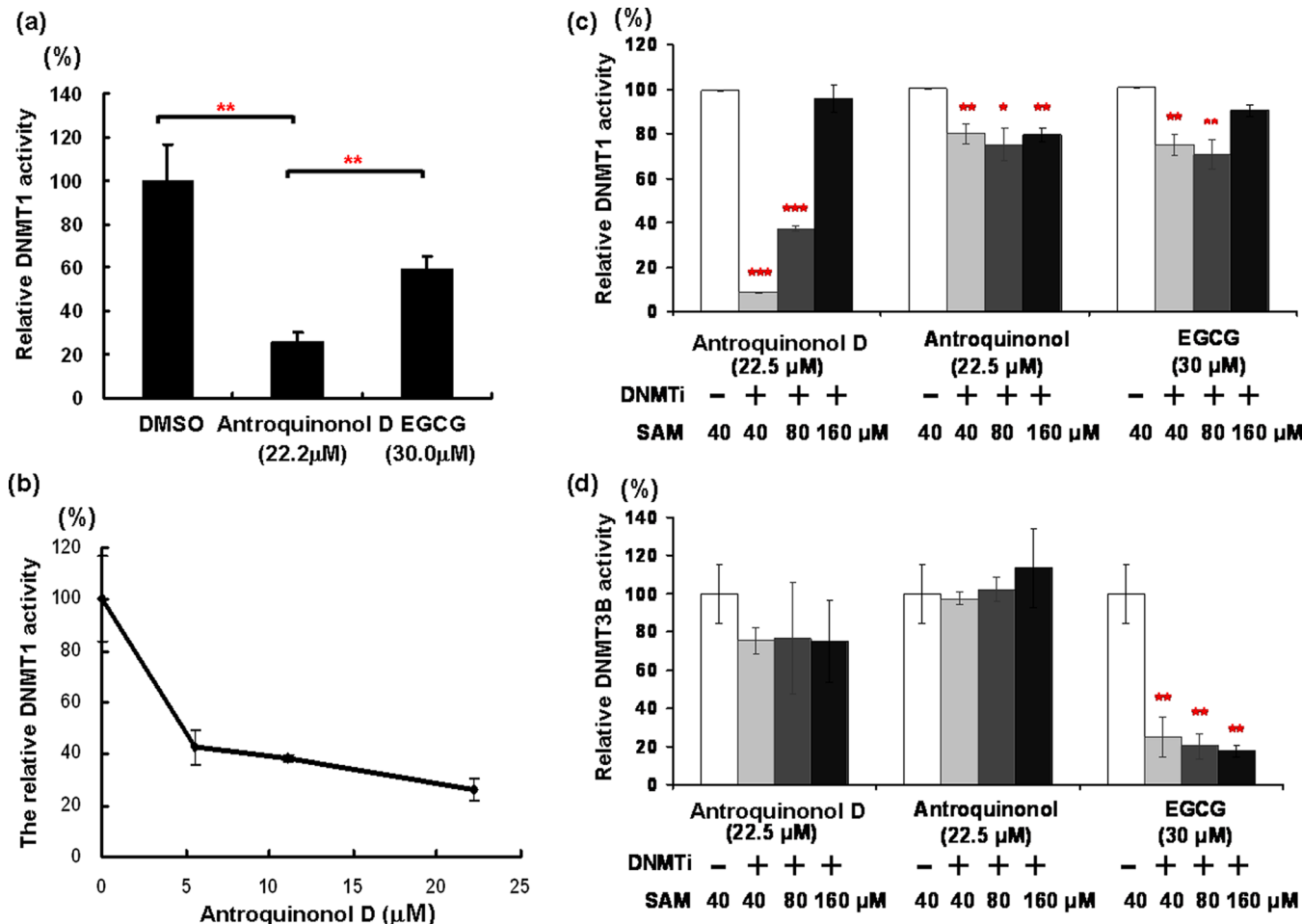


**Figure 4.** Antroquinonol D inhibits DNMT1 enzyme activity. (a) Antroquinonol D (22.5  $\mu$ M) significantly suppressed DNMT1 activity. The experiments were performed with at least three biological and three technical replicates. (b) Antroquinonol D inhibited the methylation activity of DNMT1 followed by increasing of Antroquinonol D. The DNMT1 activity assays were analyzed based on the methylation levels catalyzed by DNMT1 in the presence of either an inhibitor or the control (DMSO). EGCG was used as a positive control DNMT inhibitor. The inhibitory effects of antroquinonol D, antroquinonol or EGCG on the DNMT1 (c) or (d) DNMT3B enzymes were analyzed in the presence of 40 to 80 and 160  $\mu$ M of the cofactor SAM. \*  $p \leq 0.05$ , \*\*  $p \leq 0.005$ , \*\*\*  $p \leq 0.001$ . The data are presented as the means  $\pm$  s.d. All the experiments were performed with at least three technical replicates. The *t* test was used to calculate group differences in all experiments.

further determine whether the D-antroquinonol-mediated inhibition of cancer cell growth and migration resulted from the suppression of DNMT1 activity, we analyzed DNMT1 activity using the DNMT1 Activity/Inhibitor Screening Assay Kit. We collected natural compounds from the Graduate Institute of Pharmacognosy of Taipei Medical University, including phenolics, curcumin analogues, ubiquinone and sesquiterpene derivatives, and serially examined the DNMT1 activity. In addition to phenolics, curcumin analogues and sesquiterpene derivatives, we discovered that a ubiquinone derivative, antroquinonol D, may act as a DNMT1 inhibitor *in vitro* (Figures 1 and 4a,  $P = 0.0036$ ). Its inhibitory effects were stronger than those of the positive control DNMT inhibitor, EGCG (Figure 4a,  $P = 0.0027$ ). The IC<sub>50</sub> of antroquinonol D on DNMT1 activity was much lower than 5  $\mu$ M (Figure 4b). In addition, antroquinonol D inhibited DNMT1 activity in the presence of 40  $\mu$ M SAM. After increasing the SAM concentration from 40 to 80 and 160  $\mu$ M, the inhibitory effects of antroquinonol D on DNMT1 gradually decreased in a dose-dependent manner (Figure 4c). These results further indicate that antroquinonol D may be inserted into the putative cytosine pocket and compete with the cofactor SAM, resulting

in decreased DNMT1 activity. One antroquinonol D analogue, antroquinonol, was isolated in 2007 and was reported to be toxic to cancer cells.<sup>2</sup> Antroquinonol does not inhibit DNMT1 enzyme activity as well as antroquinonol D does (Figure 4c). For DNMT3B enzyme activity assay, antroquinonol D only slightly reduced DNMT3B enzyme activity (Figure 4d). These results may also indicate that antroquinonol D competes for the same binding pocket in the DNMT1 enzyme as SAM, but does not compete for the binding pocket in the DNMT3B enzyme (Figure 4c and d). High levels of DNMT1 mRNA and protein expression were observed in three breast cancer cell lines (MCF7, T47D and MDA-MB-231) (Figure 2f and g) that were sensitive to antroquinonol D treatment compared to normal MCF10A cells (Figure 2d and e). However, real-time RT-PCR and Western blotting analyses found that DNMT1, DNMT3A and DNMT3B mRNA and protein levels were not significantly decreased after antroquinonol D treatment (Supporting Information Figure S7).

**Molecular Modeling of the Interaction between antroquinonol D and DNMT1.** To investigate the putative mechanisms involved in the antroquinonol D-mediated inhibition of DNMT1 activity, the crystal structure of

DNMT1 in complex with sinefungin (PDB code 3SWR) was used to build the model of the human DNMT1 catalytic domain (Figure 5a). Molecular docking of antroquinonol D

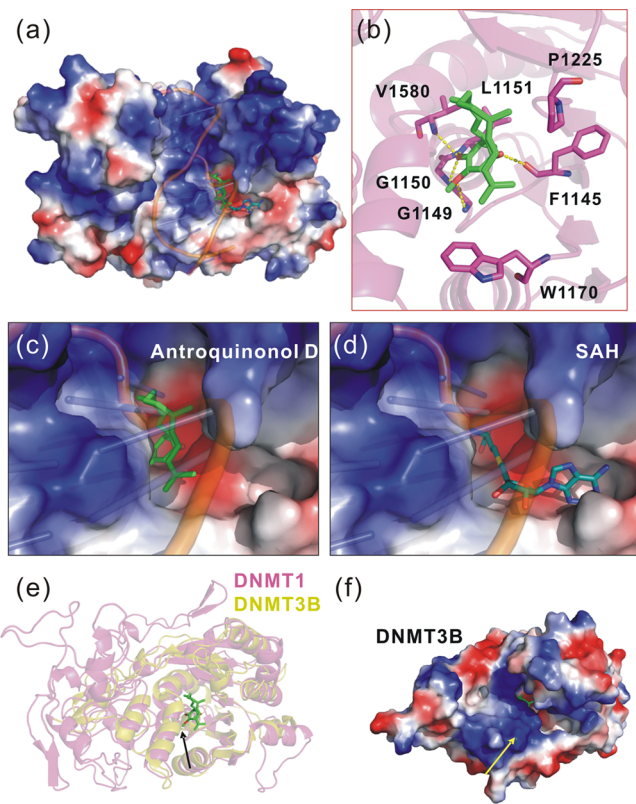


**Figure 5.** Molecular docking model of the DNMT1 catalytic domain binding to antroquinonol D or hemimethylated DNA. (a) Docking of antroquinonol D and hemimethylated DNA (brown line) in the catalytic pocket of DNMT1. (b) The binding mode of antroquinonol D upon docking to DNMT1. The hydrogen-bonding interactions of F1145, G1149, G1150, L1151 and V1580, and the van der Waals interactions with P1225 and W1170, are shown. Antroquinonol D (c) bound to the same pocket as SAH, which is the product of DNMT1 catalytic reactions (d). The ligands and site residues are shown in stick representation and colored by atom type, with the exception of the carbon atoms, which are indicated in green, cyan and purple for antroquinonol D, SAH, and the site residues, respectively. (e) Superimposition of DNMT1 (pink) and DNMT3B (yellow) structures revealed that antroquinonol D was not suitable to fit into the binding pocket of DNMT3B. (f) Bulky antroquinonol D had a crash (arrow) with the binding pocket of DNMT3B when overlapping antroquinonol D bound DNMT1 with DNMT3B.

onto the DNMT1 catalytic domain was performed. The hydrogen-bonding interactions of F1145, G1149, G1150, L1151 and V1580, and van der Waals interactions of P1225 and W1170 were observed on the residues of DNMT1 that were bound to antroquinonol D (Figure 5b). Antroquinonol D was found to bind to the same pocket as SAH, which is the SAM cofactor product of DNMT1 catalytic reactions (Figure 5c and d). DNMT3B catalytic domain was also modeled using the crystal structure of DNMT3A (PDB code 2QRV) as a template. Interestingly, when superimposing the structure of antroquinonol D bound DNMT1 with DNMT3B structure, antroquinonol D could fit into the binding pocket of DNMT3B (Figure 5e and f). The steric effect of DNMT3B on the bulky antroquinonol D entry may be the reason for the lower

inhibition ability of antroquinonol D to DNMT3B compared to DNMT1 (Figure 5e and f). The enzyme activity assay and molecular modeling of the interaction between antroquinonol D and DNMTs support that antroquinonol D selectively inhibits the DNMT1 enzyme, but not DNMT3B. The structure–activity relationships between antroquinonol and antroquinonol D with the DNMT1 enzyme was also analyzed by molecular modeling. The data showed that antroquinonol, with an additional 3'-O-CH<sub>3</sub> group, may interfere with the binding of DNMT1 more than antroquinonol D does (Supporting Information Figure S8).

#### Antroquinonol D Induces Tumor Suppressor Gene Demethylation and Re-expression in Cancer Cells.

Aberrant DNA hypermethylation of TSGs is an important mechanism underlying tumorigenesis.<sup>21,35</sup> Consequently, researchers are now searching for potential demethylating agents that can be used to reactivate TSGs in tumor cells, which may possibly lead to the suppression of cancer cell growth and invasion. To determine whether antroquinonol D can induce gene demethylation in cells, we analyzed changes in genomic methylation using the Illumina Methylation 450 K array-based assay. We discovered that treatment with 15 μM antroquinonol D for 6 days decreased the methylation status of 159 CpG sites and 113 specific genes in MDA-MB-231 breast cancer cells (Figure 6a and Supporting Information Table S2). Functional annotation clustering of differentially demethylated genes induced by following antroquinonol D treatment was performed using a Functional DAVID Bioinformatics Resources 6.7 analysis (Supporting Information Figure S9). The greatest decreases in methylation levels and increases in mRNA expression levels following antroquinonol D treatment were observed in five tumor suppressor genes: *FANCC*, *CACNA1A*, *CDH15*, *ASB9* and *COL4A2* (Figure 6a,b and Table 1). *FANCC* gene expression has been reported to be lower in stage III samples compared to stage I samples from ovarian cancer patients.<sup>36</sup> The *CACNA1A* gene encodes the α<sub>1A</sub> pore-forming subunit of Ca<sup>2+</sup> voltage-gated Cav2.1 channels. A recent report identified the *CACNA1A* gene as a novel tumor suppressor candidate that is methylated in lung cancer tumors.<sup>37</sup> Frequent promoter methylation of *CDH15* in hepatocellular carcinoma is associated with a poor prognosis.<sup>38</sup> Low expression of *ASB9* in colorectal cancer is associated with a poor prognosis.<sup>39</sup> *COL4A2* protein retards the growth of pancreatic cancer in a dose-dependent manner by inhibiting angiogenesis.<sup>40</sup> Pyrosequencing was used to further confirm the decreases in the methylation statuses of two of the tumor suppressor genes, *FANCC* and *CACNA1A*. The CpG island methylation levels in the *FANCC* and *CACNA1A* genes were decreased by approximately 9–51% and 20–51%, respectively, following antroquinonol D treatment (Figure 6c). We also used Western blotting to determine whether *FANCC* and *CACNA1A* protein expression was induced following antroquinonol D treatment. The data indicated that the *FANCC* and *CACNA1A* protein expression levels had also increased by 1.7- and 2.3-fold, respectively, following antroquinonol D treatment (Figure 6c). Note that DNA demethylation of the *ASB9* and *RPS6KA2* genes was detected using a Methylation 450 K array-based assay. However, *RPS6KA2* mRNA expression cannot be detected using real-time RT-PCR. The *ASB9* mRNA expression levels only increased 2-fold. A probable reason for these results may be that the DNA demethylation regions of *RPS6KA2* and *ASB9* were not close to the CpG islands (Table 1). Interestingly, the DNA demethylation regions of the

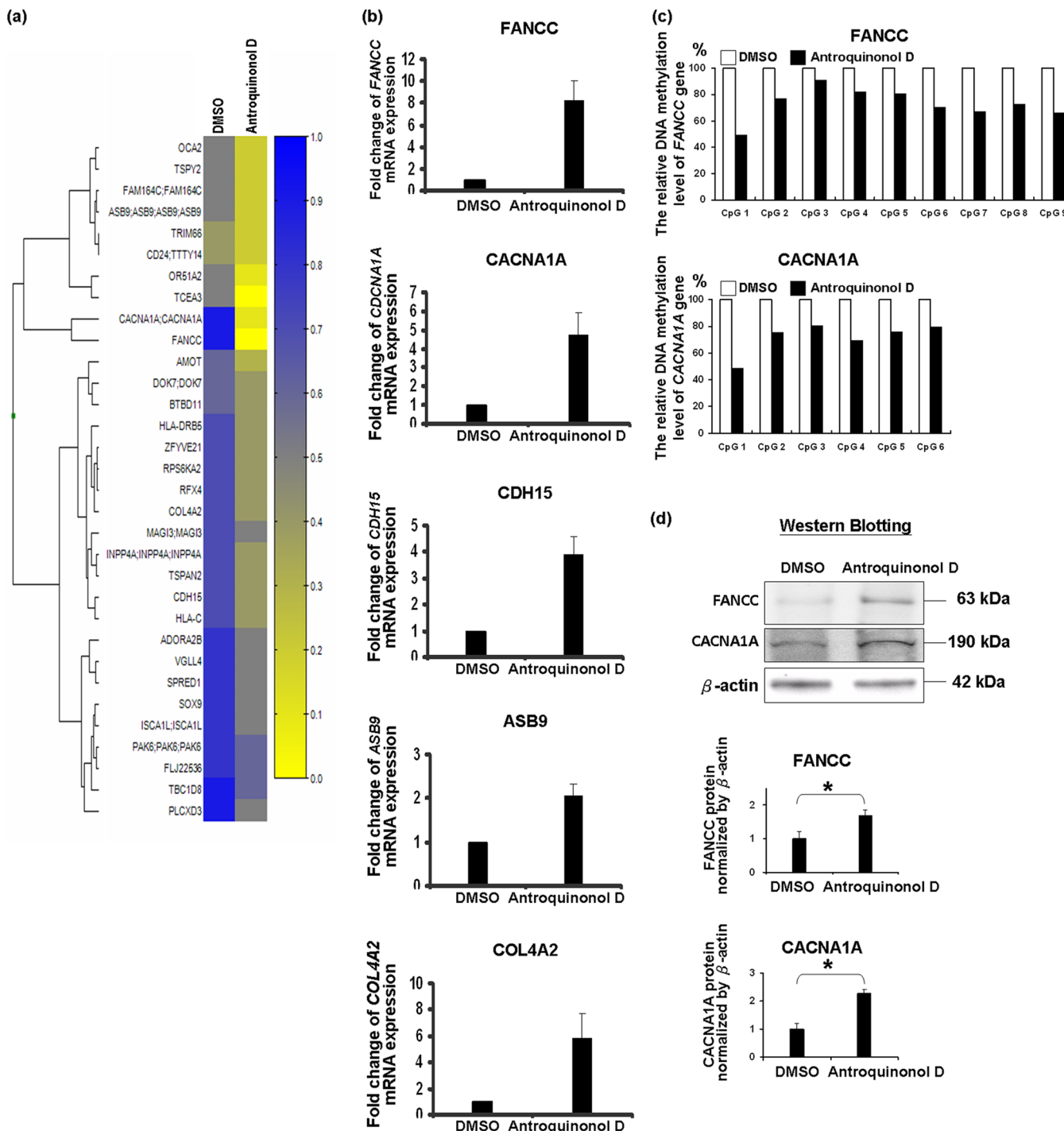


**Figure 6.** Antroquinonol D induces tumor suppressor gene demethylation and re-expression in cancer cells. (a) Methylation levels ( $\Delta\text{Avg}_\text{Beta} > 0.25$ ) at the differentially methylated loci were identified using an Illumina Methylation 450 K array-based assay following treatment with DMSO or 15  $\mu\text{M}$  antroquinonol D for 6 days in MDA-MB-231 cells and are represented on the heat map. The scale shows the relative methylation status (yellow indicates hypomethylation and blue indicates hypermethylation). (b) The mRNA levels of *FANCC*, *CACNA1A*, *CDH15*, *ASB9* and *COL4A2* were identified using real-time RT-PCR after the cells had been treated with 15  $\mu\text{M}$  antroquinonol D for 6 days. The data are presented as the means  $\pm$  s.d. Note that the DNA demethylation status of *RPS6KA2* was detected using the Methylation 450 K array-based assay. However, *RPS6KA2* mRNA expression cannot be detected using real-time RT-PCR. The experiments were performed with at least three technical replicates. (c) Pyrosequencing was used to confirm the DNA methylation status of the *FANCC* and *CACNA1A* genes following treatment with 15  $\mu\text{M}$  antroquinonol D for 6 days in MDA-MB-231 cells. (d) The protein expression levels of *FANCC* and *CACNA1A* were analyzed via Western blotting following treatment with 15  $\mu\text{M}$  antroquinonol D for 6 days. The data are presented as the means  $\pm$  s.d. \*  $P \leq 0.001$ . The experiments were performed with at least three technical replicates. The *t* test was used to calculate group differences in all experiments.

*CACNA1A*, *CDH15* and *COL4A2* genes were located within their gene bodies (Table 1). Whether those regions are important for gene expression requires further investigation.

Fewer genes were demethylated following antroquinonol D treatment than were previously reported to be demethylated following DAC treatment.<sup>41</sup> We postulated that DAC

**Table 1. Demethylation of Tumor Suppressor Genes**

demethylation ( $\Delta$ Avg_Beta) <sup>a</sup>	gene name	coverage of gene regions <sup>b</sup>	relation to CpG island <sup>c</sup>	function	reference
-0.881	FANCC	5'UTR	island shore	DNA repair	Low expression of FANCC is observed in late stage of ovarian cancer. <sup>37</sup>
-0.702	CACNA1A	gene body	island shore	calcium channels	High methylation of CACNA1A is determined in lung tumors. <sup>38</sup>
-0.323	CDH15	gene body	island shelf	cell-cell adhesion	Frequent promoter methylation of CDH15 is associated with poor prognosis in liver cancer. <sup>39</sup>
-0.277	ASB9	TSS200	no	inhibition of cytokine signaling	Low expression of ASB9 in colorectal cancer is associated with poor prognosis. <sup>40</sup>
-0.274	RPS6KA2	gene body	no	inhibition of proliferation	RPS6KA2 reduces proliferation, causes G1 arrest, increases apoptosis. <sup>43</sup>
-0.253	COL4A2	gene body	within island	inhibition of angiogenesis	COL4A2 protein retards the growth of pancreatic cancer through inhibiting angiogenesis. <sup>41,42</sup>

<sup>a</sup>Demethylation ( $\Delta$ Avg\_Beta) indicates that the change level of DNA methylation in specific gene between DMSO control and antroquinonol D treatment. The data were calculated by antroquinonol D. Avg\_Beta – DMSO.Avg\_Beta. "Beta" scores are based on the ratio of methylated signal intensity to the sum of both methylated and unmethylated signal outputs. <sup>b</sup>The relative position between DNA demethylation region and the specific tumor suppressor gene. <sup>c</sup>The relative position between DNA demethylation region and the CpG island.

incorporates into replicating DNA, inducing the chelation and degradation of the DNMT1 protein, thereby preventing DNA methylation. Therefore, the mechanism underlying antroquinonol D-mediated DNMT1 inhibition differs from that of DAC and AZA, and therefore, antroquinonol D may be used as an alternative DNMT inhibitor. Antroquinonol D may induce far fewer cytotoxic effects than DAC because only certain genes are demethylated following antroquinonol D treatment. Therefore, antroquinonol D may still be worth optimizing to generate a more specific DNMT inhibitor.

In conclusion, we identified a new DNMT1 inhibitor, antroquinonol D, which induced DNA demethylation and reversed the silencing of multiple tumor suppressor genes, induced cancer cell death and inhibited cell migration. Further investigation of antroquinonol D using molecular biochemistry assays, animal studies, pharmacokinetics assays and clinical studies is required to determine whether antroquinonol D can be used clinically.

## ASSOCIATED CONTENT

### Supporting Information

The Supporting Information includes the DNMT1 inhibitor treatment protocols for the cells; the viability and cytotoxicity of breast cells after DNMT inhibitors treatment; images presenting morphological changes in MDA-MB-231 cells; Expression levels of DNMTs following antroquinonol D treatment; antroquinonol D effects on the AKT pathway; functional annotation clustering; the growth curves of cells over 6 days, assayed by Sulforhodamine B; a list of primer sequences and their reaction conditions used in the present study; the demethylation in genes. This material is available free of charge via the Internet at <http://pubs.acs.org>.

## AUTHOR INFORMATION

### Corresponding Author

\*Tel.: +886 2 27361661, ext. 6162. Fax: +886 2 27361661, ext. 6162. E-mail: linruokai@tmu.edu.tw.

### Funding

This work was supported in part by grant TMU99-AE1-B21 from the Taipei Medical University and grants NSC100–2320-B-038-002, NSC100–2320-B-038-014 and NSC99-2119-M-002-010 from the National Science Council (Republic of China).

## Notes

The authors declare no competing financial interest.

## ABBREVIATIONS USED

*A. camphorata*, *Antrodia camphorata*; ASB9, ankyrin repeat and SOCS box containing 9; Antroquinonol D, 3-demethoxyl antroquinonol; AZA, 5-azacytidine; DAC, 5-aza-2'-deoxycytidine (decitabine); BCRC, Bioresource Collection and Research Center; CACNA1A, calcium channel voltage-dependent P/Q type alpha 1A subunit; CDH15, cadherin 15 type 1 M-cadherin; CI, Cell Index; COL4A2, collagen type IV alpha 2; DNMT1, DNA methyltransferase 1; EGCG, epigallocatechin-3-gallate; TSG, tumor suppressor gene; FANCC, fanconi anemia complementation group C; F-actin, filamentous actin; GI50, 50% growth inhibition; NMR, Nuclear magnetic resonance; SAM, S-adenosyl methionine; FDA, US Food and Drug Administration; SDS, sodium dodecyl sulfate; SRB, Sulforhodamine B

## REFERENCES

- (1) Geethangili, M.; Tzeng, Y. M. Review of pharmacological effects of *Antrodia camphorata* and its bioactive compounds. *Evid. Based Complement. Alternat. Med.* **2011**, *2011*, 212641.
- (2) Lee, T. H.; Lee, C. K.; Tsou, W. L.; Liu, S. Y.; Kuo, M. T.; Wen, W. C. A new cytotoxic agent from solid-state fermented mycelium of *Antrodia camphorata*. *Planta Med.* **2007**, *73*, 1412–5.
- (3) Nakamura, N.; Hirakawa, A.; Gao, J. J.; Kakuda, H.; Shiro, M.; Komatsu, Y.; Sheu, C. C.; Hattori, M. Five new maleic and succinic acid derivatives from the mycelium of *Antrodia camphorata* and their cytotoxic effects on LLC tumor cell line. *J. Nat. Prod.* **2004**, *67*, 46–8.
- (4) Sekido, Y.; Fong, K. M.; Minna, J. D. Progress in understanding the molecular pathogenesis of human lung cancer. *Biochim. Biophys. Acta* **1998**, *1378*, F21–59.
- (5) Jovanovic, J.; Ronneberg, J. A.; Tost, J.; Kristensen, V. The epigenetics of breast cancer. *Mol. Oncol.* **2010**, *4*, 242–54.
- (6) Nephew, K. P.; Huang, T. H. Epigenetic gene silencing in cancer initiation and progression. *Cancer Lett.* **2003**, *190*, 125–33.
- (7) Belinsky, S. A. Gene-promoter hypermethylation as a biomarker in lung cancer. *Nat. Rev. Cancer* **2004**, *4*, 707–17.
- (8) Jamaluddin, M. S.; Yang, X.; Wang, H. Hyperhomocysteinemia, DNA methylation and vascular disease. *Clin. Chem. Lab. Med.* **2007**, *45*, 1660–6.
- (9) Costa, E.; Dong, E.; Grayson, D. R.; Guidotti, A.; Ruzicka, W.; Veldic, M. Reviewing the role of DNA (cytosine-5) methyltransferase overexpression in the cortical GABAergic dysfunction associated with psychosis vulnerability. *Epigenetics* **2007**, *2*, 29–36.

- (10) Egger, G.; Liang, G.; Aparicio, A.; Jones, P. A. Epigenetics in human disease and prospects for epigenetic therapy. *Nature* **2004**, *429*, 457–63.
- (11) Rhee, I.; Bachman, K. E.; Park, B. H.; Jair, K. W.; Yen, R. W.; Schuebel, K. E.; Cui, H.; Feinberg, A. P.; Lengauer, C.; Kinzler, K. W.; Baylin, S. B.; Vogelstein, B. DNMT1 and DNMT3b cooperate to silence genes in human cancer cells. *Nature* **2002**, *416*, 552–6.
- (12) Mastroeni, D.; Grover, A.; Delvaux, E.; Whiteside, C.; Coleman, P. D.; Rogers, J. Epigenetic changes in Alzheimer's disease: decrements in DNA methylation. *Neurobiol. Aging* **2010**, *31*, 2025–37.
- (13) De Marzo, A. M.; Marchi, V. L.; Yang, E. S.; Veeraswamy, R.; Lin, X.; Nelson, W. G. Abnormal regulation of DNA methyltransferase expression during colorectal carcinogenesis. *Cancer Res.* **1999**, *59*, 3855–60.
- (14) Lin, R. K.; Hsu, H. S.; Chang, J. W.; Chen, C. Y.; Chen, J. T.; Wang, Y. C. Alteration of DNA methyltransferases contributes to 5' CpG methylation and poor prognosis in lung cancer. *Lung Cancer* **2007**, *55*, 205–13.
- (15) Girault, I.; Tozlu, S.; Lidereau, R.; Bieche, I. Expression analysis of DNA methyltransferases 1, 3A, and 3B in sporadic breast carcinomas. *Clin. Cancer Res.* **2003**, *9*, 4415–22.
- (16) Saito, Y.; Kanai, Y.; Nakagawa, T.; Sakamoto, M.; Saito, H.; Ishii, H.; Hirohashi, S. Increased protein expression of DNA methyltransferase (DNMT) 1 is significantly correlated with the malignant potential and poor prognosis of human hepatocellular carcinomas. *Int. J. Cancer* **2003**, *105*, 527–32.
- (17) Ethoh, T.; Kanai, Y.; Ushijima, S.; Nakagawa, T.; Nakanishi, Y.; Sasako, M.; Kitano, S.; Hirohashi, S. Increased DNA methyltransferase 1 (DNMT1) protein expression correlates significantly with poorer tumor differentiation and frequent DNA hypermethylation of multiple CpG islands in gastric cancers. *Am. J. Pathol.* **2004**, *164*, 689–99.
- (18) Mizuno, S.; Chijiwa, T.; Okamura, T.; Akashi, K.; Fukumaki, Y.; Niho, Y.; Sasaki, H. Expression of DNA methyltransferases DNMT1, 3A, and 3B in normal hematopoiesis and in acute and chronic myelogenous leukemia. *Blood* **2001**, *97*, 1172–9.
- (19) Qiu, X.; Zhang, L.; Lu, S.; Song, Y.; Lao, Y.; Hu, J.; Fan, H. Upregulation of DNMT1 mediated by HBx suppresses RASSF1A expression independent of DNA methylation. *Oncol. Rep.* **2014**, *31*, 202–8.
- (20) Issa, J. P.; Garcia-Manero, G.; Giles, F. J.; Mannari, R.; Thomas, D.; Faderl, S.; Bayar, E.; Lyons, J.; Rosenfeld, C. S.; Cortes, J.; Kantarjian, H. M. Phase 1 study of low-dose prolonged exposure schedules of the hypomethylating agent 5-aza-2'-deoxycytidine (decitabine) in hematopoietic malignancies. *Blood* **2004**, *103*, 1635–40.
- (21) Esteller, M. Dormant hypermethylated tumour suppressor genes: questions and answers. *J. Pathol.* **2005**, *205*, 172–80.
- (22) Lubbert, M.; Suciu, S.; Baila, L.; Ruter, B. H.; Platzbecker, U.; Giagounidis, A.; Selleslag, D.; Labar, B.; Germing, U.; Salih, H. R.; Beeldens, F.; Muus, P.; Pfluger, K. H.; Coens, C.; Hagemeijer, A.; Eckart Schaefer, H.; Ganser, A.; Aul, C.; de Witte, T.; Wijermans, P. W. Low-dose decitabine versus best supportive care in elderly patients with intermediate- or high-risk myelodysplastic syndrome (MDS) ineligible for intensive chemotherapy: final results of the randomized phase III study of the European Organisation for Research and Treatment of Cancer Leukemia Group and the German MDS Study Group. *J. Clin. Oncol.* **2011**, *29*, 1987–96.
- (23) Medina-Franco, J. L.; Caulfield, T. Advances in the computational development of DNA methyltransferase inhibitors. *Drug Discovery Today* **2011**, *16*, 418–25.
- (24) Lin, R. K.; Hsu, C. H.; Wang, Y. C. Mithramycin A inhibits DNA methyltransferase and metastasis potential of lung cancer cells. *Anticancer Drugs* **2007**, *18*, 1157–64.
- (25) Strelmann, C.; Brueckner, B.; Musch, T.; Stopper, H.; Lyko, F. Functional diversity of DNA methyltransferase inhibitors in human cancer cell lines. *Cancer Res.* **2006**, *66*, 2794–800.
- (26) Monto, R. W.; Talley, R. W.; Caldwell, M. J.; Levin, W. C.; Guest, M. M. Observations on the mechanism of hemorrhagic toxicity in mithramycin (NSC 24559) therapy. *Cancer Res.* **1969**, *29*, 697–704.
- (27) Morris, G. M.; Huey, R.; Olson, A. J., Using AutoDock for ligand-receptor docking. *Curr. Protoc. Bioinform.* **2008**, Chapter 8, Unit 8.14.
- (28) Huey, R.; Morris, G. M.; Olson, A. J.; Goodsell, D. S. A semiempirical free energy force field with charge-based desolvation. *J. Comput. Chem.* **2007**, *28*, 1145–52.
- (29) Mosmann, T. Rapid colorimetric assay for cellular growth and survival: application to proliferation and cytotoxicity assays. *J. Immunol. Methods* **1983**, *65*, 55–63.
- (30) Wei, P. L.; Kuo, L. J.; Wang, W.; Lin, F. Y.; Liu, H. H.; How, T.; Ho, Y. S.; Huang, M. T.; Wu, C. H.; Chang, Y. J. Silencing of glucose-regulated protein 78 (GRP78) enhances cell migration through the upregulation of vimentin in hepatocellular carcinoma cells. *Ann. Surg. Oncol.* **2012**, *19* (Suppl 3), S72–9.
- (31) Huang da, W.; Sherman, B. T.; Lempicki, R. A. Systematic and integrative analysis of large gene lists using DAVID bioinformatics resources. *Nat. Protoc.* **2009**, *4*, 44–57.
- (32) Li, L. C.; Dahiya, R. MethPrimer: designing primers for methylation PCRs. *Bioinformatics* **2002**, *18*, 1427–31.
- (33) Stricker, J.; Falzone, T.; Gardel, M. L. Mechanics of the F-actin cytoskeleton. *J. Biomech.* **2010**, *43*, 9–14.
- (34) Yu, C. C.; Chiang, P. C.; Lu, P. H.; Kuo, M. T.; Wen, W. C.; Chen, P.; Guh, J. H. Antroquinonol, a natural ubiquinone derivative, induces a cross talk between apoptosis, autophagy and senescence in human pancreatic carcinoma cells. *J. Nutr. Biochem.* **2012**, *23*, 900–7.
- (35) Momparler, R. L. Cancer epigenetics. *Oncogene* **2003**, *22*, 6479–83.
- (36) Ganzinelli, M.; Mariani, P.; Cattaneo, D.; Fossati, R.; Frusci, R.; Corso, S.; Ricci, F.; Broggini, M.; Damia, G. Expression of DNA repair genes in ovarian cancer samples: biological and clinical considerations. *Eur. J. Cancer* **2011**, *47*, 1086–94.
- (37) Castro, M.; Grau, L.; Puerta, P.; Gimenez, L.; Venditti, J.; Quadrelli, S.; Sanchez-Carbayo, M. Multiplexed methylation profiles of tumor suppressor genes and clinical outcome in lung cancer. *J. Transl. Med.* **2010**, *8*, 86.
- (38) Yamada, S.; Nomoto, S.; Fujii, T.; Takeda, S.; Kanazumi, N.; Sugimoto, H.; Nakao, A. Frequent promoter methylation of M-cadherin in hepatocellular carcinoma is associated with poor prognosis. *Anticancer Res.* **2007**, *27*, 2269–74.
- (39) Tokuoka, M.; Miyoshi, N.; Hitora, T.; Mimori, K.; Tanaka, F.; Shibata, K.; Ishii, H.; Sekimoto, M.; Doki, Y.; Mori, M. Clinical significance of ASB9 in human colorectal cancer. *Int. J. Oncol.* **2010**, *37*, 1105–11.
- (40) He, X. P.; Li, Z. S.; Zhu, R. M.; Tu, Z. X.; Gao, J.; Pan, X.; Gong, Y. F.; Jin, J.; Man, X. H.; Wu, H. Y.; Xu, A. F. Effects of recombinant human canstatin protein in the treatment of pancreatic cancer. *World J. Gastroenterol.* **2006**, *12*, 6652–7.
- (41) Tsai, H. C.; Li, H.; Van Neste, L.; Cai, Y.; Robert, C.; Rassool, F. V.; Shin, J. J.; Harbom, K. M.; Beaty, R.; Pappou, E.; Harris, J.; Yen, R. W.; Ahuja, N.; Brock, M. V.; Stearns, V.; Feller-Kopman, D.; Yarmus, L. B.; Lin, Y. C.; Welm, A. L.; Issa, J. P.; Minn, I.; Matsui, W.; Jang, Y. Y.; Sharkis, S. J.; Baylin, S. B.; Zahnow, C. A. Transient low doses of DNA-demethylating agents exert durable antitumor effects on hematological and epithelial tumor cells. *Cancer Cell* **2012**, *21*, 430–46.
- (42) Bignone, P. A.; Lee, K. Y.; Liu, Y.; Emilion, G.; Finch, J.; Soosay, A. E.; Charnock, F. M.; Beck, S.; Dunham, I.; Mungall, A. J.; Ganesan, T. S. RPS6KA2, a putative tumour suppressor gene at 6q27 in sporadic epithelial ovarian cancer. *Oncogene* **2007**, *26*, 683–700.